Heliyon 5 (2019) e02557

Contents lists available at ScienceDirect

Heliyon

journal homepage: www.heliyon.com

Heliyon

Review article

Micro-computed tomographic and SEM study of porous bioceramics using an adaptive method based on the mathematical morphological operations

M. Ezzahmouly [a,*], A. Elmoutaouakkil [a], M. Ed-Dhahraouy [a], H. Khallok [b], A. Elouahli [b], A. Mazurier [c], A. ElAlbani [c], Z. Hatim [b]

[a] Research Laboratory in Optimization, Emerging Systems, Networks and Imaging, LAROSERI, Computer Science Department, ChouaïbDoukkali University, Eljadida, Morocco
[b] Electrochemical and Biomaterials Team, Chemistry Department, ChouaïbDoukkali University, Eljadida, Morocco
[c] IC2MP, UMR CNRS 7285, Poitiers University, Poitiers, France

ARTICLE INFO

Keywords:
Computer science
Materials science
Pharmaceutical chemistry
Morphological operations
Image processing
Biomaterials
Microstructural analysis
Medical information systems
Data analysis
Data visualization
Computational materials science
Materials characterization
Materials structure
Microstructure

ABSTRACT

Numerous clinical studies have demonstrated the influence of the size, number and shape of pores into calcium phosphate ceramics on the process of bone regeneration.

The main objective of this study is to determine the microstructure, the morphological characteristics and classes of pores of the prepared hydroxyapatite bioceramic using an adaptive method based on the mathematical morphological operations. The study was carried out using X-ray microtomography and Scanning Electron Microscopy images. The conventional method of openings alone presents limitation of calculation and not sufficient to achieve our objective. The proposed method allowed us to extract local characteristics and calculate precisely the morphological parameters while preserving the original volume of pores. The number and classes of pores with their size, surface of contact of the component and the number of connected pores to each pore were calculated. The method is subjectively and quantitatively evaluated using different computed phantoms and its efficiency is clearly demonstrated through the different reports and measurements generated. The proposed method can have interesting applications in the characterization of porous materials used in the medical field or in other sectors.

1. Introduction

In the domain of orthopaedic surgery, traumatic situations lead to bone loss, following either a fracture, a congenital disease or a cancer. These bone losses have consolidation problems which require the use of either bone grafts or implants that present themselves as an alternative to transplants [1, 2, 3]. These implants are usually made of metal, polymer or ceramic, and are either biodegradable or not. At present, calcium hydroxyapatite ($(Ca_{10}(PO_4)_6(OH)_2$: HAP) ceramics are very attractive biomaterials as bone substitute materials due to their excellent biocompatibility, bioactivity and osteoconduction (The process by which bone grows on a ceramic surface.) properties [4, 5, 6].

Depending on the desired application, these biomaterials exist in several porous forms as granules or blocks [7]. Volume porosity and pore size affect the ability of the scaffold to promote vascularization, cells proliferation and in vivo osteoconduction. It has been established that pore sizes of at least 40 μm are required for bone ingrowth, whereas interconnected pores larger than 100 μm in diameter are required to promote the integration of the implant. Characterization of the porous architecture of scaffolds is essential in predicting their performance in vivo [8]. Several processing methods have recently been used for porosity study. However, many of them can't be used to quantify the closed porosity, inaccessible by external agents (mercury, nitrogen, argon...).

Compared to these older methods, Scanning Electron Microscopy (SEM) analysis can give an idea of the two dimensional relief microstructure and micro computed tomography (μCT) analysis is today considered as the three dimensional method for rapid non-destructive microstructural analysis of biomaterials [9].

To exploit and evaluate the microstructure from SEM and μCT images, several image-processing methods should be exploited and adapted efficiently depending on the desired information. Image processing is

* Corresponding author.
E-mail address: ezzahmoulymnl@gmail.com (M. Ezzahmouly).

https://doi.org/10.1016/j.heliyon.2019.e02557
Received 16 September 2018; Received in revised form 3 July 2019; Accepted 27 September 2019

then a crucial step in the quantification of porous structures.

Edges and corners are regions of interest where there is an unexpected change in intensity. These features play an important role in object identification methods utilized in machine vision and image processing systems [10, 11]. Therefore; by distinguishing edges in an image precisely, every objects can be found and essential properties for example area, border and shape can be estimated.

Binary images may contain various flaws. Specifically, the double areas created by basic thresholding are distorted by noise and texture. Morphology identifies with structure or form of items [11, 12]. Therefore, Mathematical morphological operations are used to analyze region shapes.

Mathematical morphology is a mathematical discipline established in the 1960's [13, 14]. It depends on set theory and studies the geometrical structure of an image by coordinating it with the structuring component at different areas in the image. By changing the size and the shape of structuring components, geometrical data of the various items of the image and their interrelation can be extracted, for example, boundaries, skeletons, and the convex structure, which can encourage shape investigation [15, 16].

The method has additionally been utilized for preprocessing and post-processing, for example, morphological filtering, thinning and pruning. Different applications have been investigated with this innovation, for example, watershed transformation [17]. Gauch et al. [18] exhibited a way to deal with image segmentation and analysis by utilizing multi-scale gradient watershed hierarchies. Nedzved et al. [19] developed fast gray-scale thinning algorithm to segment histology cell images. A more detailed review of segmentation of range images utilizing morphological operations can be found in the literature [20, 21].

Since the element moves across the images, some complex ones may not be processed efficiently. As a result, an artefact can be induced at the object periphery or squarely the whole shape changes [22, 23]. Another issue consists on the separation of connected pores while preserving the irregular shape of the initial pore. The use of the conventional method leads to loose small connected pores, which causes the deformation of the original shape of the pore. Therefore a bad quantitate porosity study is generated. Those drawbacks are especially serious problems, since pores in biomaterial samples consist of delicate structural features.

To overcome those issues and unlike existing techniques expressly utilizing morphological activities to disintegrate images, our strategy uses multi-scale morphological information and task to gather neighbourhood shape data and use it with the original information to facilitate volume division and evaluation of pores. An adaptive method based on mathematical morphology algorithm is proposed then in order to efficiently segment and characterize the porosity structure.

Porous calcium-hydroxyapatite ceramics prepared from cement paste was used and the microstructure of ceramic was examined by SEM and μCT.

The proposed method is used for local features extraction and calculation of morphological parameters while preserving the original volume of pores. The method is subjectively and quantitatively evaluated using different computed phantoms and its efficiency is demonstrated through the different reports and measurements generated.

2. Main text

2.1. Materials and methods

2.1.1. Porous calcium-hydroxyapatite ceramic

Hydroxyapatite Ceramic ($Ca_{10}(PO_4)_6(OH)_2$: HAP) was prepared from cement paste according to the method described by J.L.Lacout, and all [24] with some modifications. The cement was prepared by mixing tetra-calcium powder ($Ca_4(PO_4)_2O$: (TTCP)) with aqueous solution of phosphoric acid (H_3PO_4), calcium chloride ($CaCl_2$, $2H_2O$) and lactic acid ($C_3H_6O_3$). The molar ratio Ca/P of mixture was 1.667 (molar ratio of the stoichiometric hydroxyapatite) and the liquid (L) to solid (S) ratio (L/S) according to 0.55 ml g^{-1}. The mixture was done manually in a mortar with a pestle for 2 min. In order to produce the pores in the prepared material, H_2O_2solution was mixed with the fresh material paste. All of the used reagents are of analytical grade.

Cement pellets were then prepared by filling cylindrical silicone moul dwith the prepared paste. The parts were then placed in water at 80 °C for 24 h. After drying, pellets are demoulded and calcined at 1200 °C for 3 h. Photography of Fig. 1 shows the microstructure of prepared porous ceramic.

2.1.2. Image techniques

2.1.2.1. Scanning electron microscopy. The scanning electron microscope (SEM) utilizes a focused beam of high-energy electrons to create an assortment of signals at the outside of solid samples. The signals that get from electron-sample interactions expose information about the sample including outer morphology (texture), elementary chemical composition, and crystalline structure and orientation of materials.

2.1.2.1.1. SEM imaging process.

- Electron gun creates high energy electrons which are engaged into a fine beam, which is scanned across the outside of the sample.
- Elastically and inelastic interactions of the beam electrons with the atoms of the sample produce a wide assortment of radiation items like backscattered electrons, secondary electrons, absorbed electrons, characteristic and continuum x-rays (Fig. 2).
- The electrons that can be gathered by the detectors are frequently emitted at a depth of less than 10 nanometres.
- A sample of this radiation is gathered by a detector, most usually the Everhart—Thornley detector and the gathered signal is enhanced and showed on the computer
- The SEM image is produced. It is a 2D intensity map in the analog or digital domain. Each image pixel on the presentation relates to a point on the sample, which is corresponding to the signal intensity caught by the detector at every particular point [25].

The calcium-hydroxyapatite ceramic was analysed by Scanning Electron Microscope using a high-resolution device (SEM, JEOL JSM-5300), operating at 15 kV).

2.1.2.2. X-ray microtomography. Microtomography uses X-rays to create cross-sections of a physical object that can be used to reconstitute a virtual model without destroying the original object [26].

The Beer-Lambert law is the linear relationship between absorbance and concentration of an absorbing species. The Fig. 3 illustrates the principle of tomography.

The exponential attenuation law of Lambert-Beer is represented by

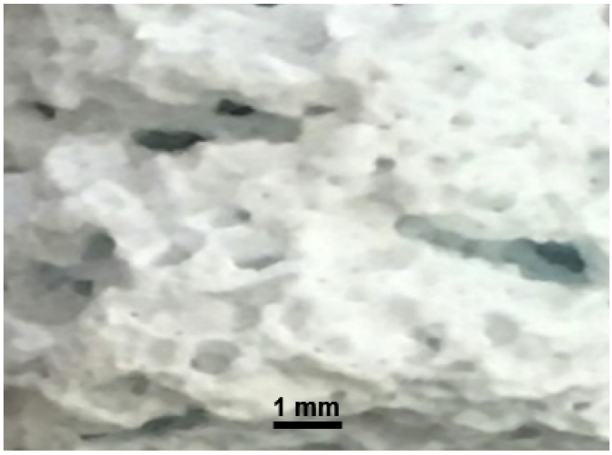

Fig. 1. Photography of porous calcium-hydroxyapatite ceramic.

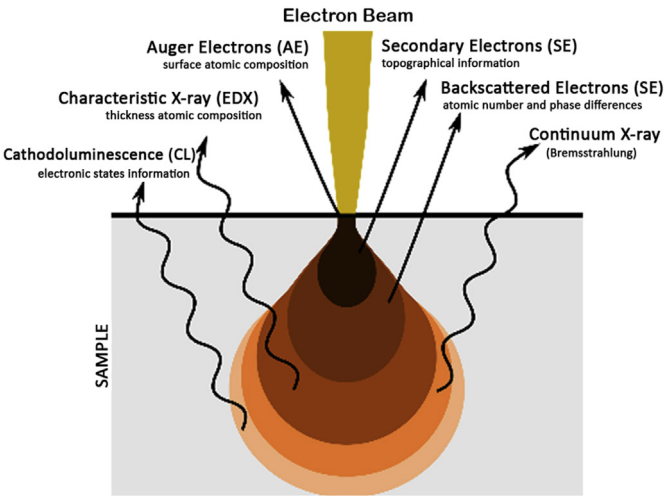

Fig. 2. Effects produced by electron-beam interaction with a specimen.

the Eq. (1)

$$I = I_0 \exp(-\mu x) \quad (1)$$

I– the intensity of light. μ– the linear attenuation coefficient [27].

Image reconstruction is the phase in which the scan data set is processed to produce an image:

- The scan data phase produces a data set, named sinogram.
- Filtered back projection is the reconstruction method used in μCT.
- The image reconstruction phase produces an image from the scan data set by the process of filtered back projection [28].

The calcium-hydroxyapatite ceramic was submitted to a computed microtomograph (μCT) using a high-resolution device (EasyTom XL duo (2 sources)). The pixel size was determined at 10.38 μm under the following conditions: 90 kV, 111 mA. About 1331 cuts were generated. The reconstructed images were processed with XAct (RX solution) software.

2.1.3. *Image processing method*

2.1.3.1. Description of the method. The objective of our work is to carry out a qualitative and quantitative evaluation of the porous microstructure of HAP bio-ceramic using SEM and μCT images.

An accurate method is proposed to characterize pores and separate them at the same time. The method makes it possible to easily calculate many quantitative measurements, in particular those that provide information on the connection and the size distribution of the pores.

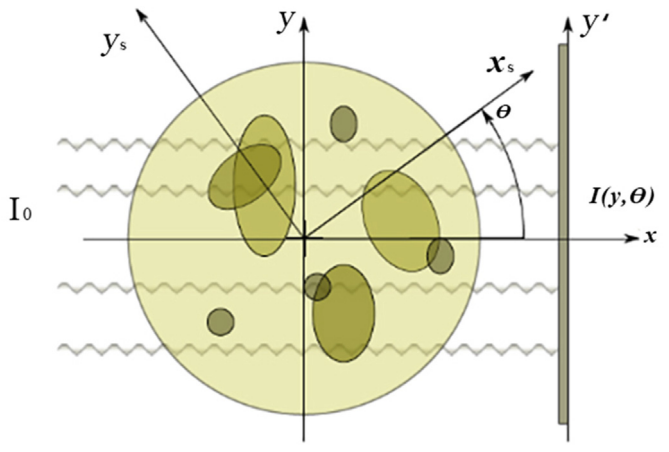

Fig. 3. Illustrated principle of tomography.

To realize those tasks, an adaptive method based on the morphological operation algorithm is proposed. The conventional method of openings alone is not sufficient to achieve our objective. It presents incorrect separations of the pores, imprecise volumes of each pore and therefore a limitation of calculations.

The proposed method lets us to calculate precisely a specific porosity and define classes of porosity.

We proceed first by the pre-processing step applied on SEM and μCT images. Fig. 4a shows SEM image and Fig. 4b shows a μCT slice image of prepared ceramic.

The median filter is used to operate local mitigations that fade near the edges. It thus eliminates the occasional noise by increasing the contrast near the edges and enhances structures [29].

To separate the pores structure from the rest of sample, we carefully choose the threshold. It converts a gray-scale image into a binary image where the two levels are assigned to pixels that are below or above the specified threshold value [30].

It is useful to be able to separate out the regions of the image corresponding to pores which interests us from the rest of sample. However, the simple threshold does not allow separating pores between them depending on their size.

Mathematical Morphology has been broadly used in image processing and shape analysis of features of interest [31]. The fundamental morphological set operations consist of union, intersection and complement. The operands of the set operations are the original data and data translated from the original with a reference shape called a structuring element [32].

A structuring element can be formed by a set of vectors. Then the fundamental mathematical morphological operations called dilation and erosion can be defined with the basic Minkowski set operations called addition and subtraction [33].

Erosion of an image I by the structure element H is given by the set operation (Eq. (2))

$$I \ominus H = \{p \in Z^2 | (p+q) \in I, for\ every\ q \in H\} = \bigcap_{q \in H} I_{-q} \quad (2)$$

- Dilation of an image I by the structure element H is given by the set operation

$$I \oplus H = \{(p+q) | p \in I, q \in H\} = \bigcup_{p \in I} H_p = \bigcup_{q \in H} I_q \quad (3)$$

Holes in the foreground that are smaller than H will be filled.

Erosion reduces the size of the pores by eroding its outline and dilation by dilating its outline, with the predefined structure element. Erosion followed by dilation is called opening [34].

They are mathematical morphology tools that process images based usually on shapes and most commonly change them. Those operations affect directly the efficiency of pores measurements especially those with an irregular shape.

For an efficient porosity study, it is useful to separate the pores from one another and label them. This allows us to calculate many parameters mainly the volume, the apparent perimeter and the surface contact.

Moreover, the conventional method based on openings alone is inappropriate for an efficient quantitative analysis. This approach does not take into account convexity hypotheses on the forms encountered and does not divide them to achieve a distribution of the separated pores.

To surpass those limits, a method based on the use of morphological operations is proposed. Successive openings operations are computed with structuring element increasing in diameter to make the particles disappear progressively. The difference between the images before and after an opening, corresponds to the total volume of the particles disappeared. The volume and the contact area of the isolated elements are

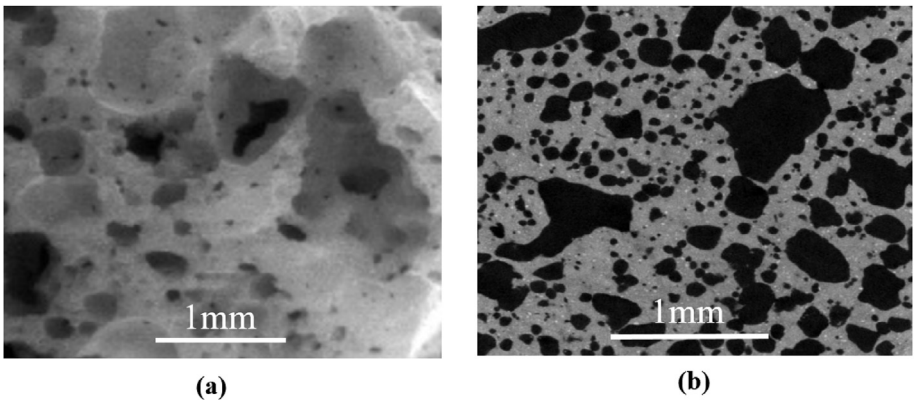

Fig. 4. (a) SEM image, (b) μCT slice image of HAP ceramic.

calculated with the original element. This calculation is done via a voxel/pixel path in the subtracted image. Neighbouring voxels/pixels of components are compared; a voxel/pixel having different gray level value neighbours in the original image is indeed a contact surface.

A component may be connected with more than one other component. The method allows us to calculate for each component, the number of contacts (Nsc) with other interfaces.

After those operations, the small elements and the corners belonging to the pore, which are found in the reference image, disappear.

The conventional method considers them as distinct components, but the originality of our method is that it does not take them into account on the basis of a geometric criterion. The contact surface, the number of contact surfaces with the other elements, and the total and specific pore volume will be calculated.

Since the structuring element of the conventional method moves across the image, some intricate images may not be properly processed. Consequently, an artefact in the shape of structural elements may be generated at the object periphery or squarely the periphery shape changes that leads also directly to a bad quantitative study. To overcome this, the analyses are carried out on the contact surface; if it is larger than the surface area of the subtracted element, the element is left with its original structure otherwise, it is not taken into account in the calculation of the porosity. We then solve the problem of small connected structures considered as a single pore which disappears after the opening. Fig. 5 illustrates the flowchart of the proposed method to calculate porosity parameters.

2.1.3.2. Validation of the proposed method. To validate our method, phantoms with spheres with different sizes and the irregular shape are computed (Fig. 6).

The phantom with different sphere sizes (Fig. 6a) is used to validate how the method is statistically precise and able to keep the shape of the original structure. Contrary to the conventional method, the proposed one should not intrigued the volume of a larger sphere in the calculation of a smaller sphere.

The microstructure includes the pores with non-regular shapes and interconnected pores. The goal is to keep the small pores stuck to the great structure by considering it all as a single pore. Another objective is to separate the connected pores. Hence the choice of such a phantom containing the different cases (Fig. 6b).

In this case, the method should consider the component A part of the square component and the component B as another element. The component B should be separated from the adjacent structure (square component + component A) and be counted as a pore apart with a volume, its surface contact with the adjacent structure will be determined as well.

The method had been applied to the computed phantoms. The total volume pore (Vp) and total porosity (P) (%) were calculated.

2.1.3.3. Error estimation. To evaluate the accuracy of our method, the absolute error value of the conventional opening method and the proposed one was calculated and then the Mean Absolute Error (MAE) value was determined [35].

Absolute error (*e*) is the difference between the measured value and the actual value. It is one way to consider error when measuring the accuracy of values.

$$e = x_o - x \tag{4}$$

Where e – the absolute error (the difference, or change, in the measured and actual value), x_o– the measured value, and x– the actual value.

Mean absolute error (MAE**)** is a measure of difference between two variables. It is expressed as

$$MAE = \sum_{i=1}^{n} |e_i| \Big/ n \tag{5}$$

Where n– number of variables.

2.2. Results and discussion

After applying the filtering and thresholding, the proposed method is applied as described in the method section to separate pores while preserving their shape. This allows us to calculate many numerical parameter values of the sample especially the number of pores with their size, surface of contact of the component and the number of connected pores to each pore.

2.2.1. Phantoms study

2.2.1.1. Phantom of spheres with different sizes. The conventional method of opening and the proposed method are applied on the computed phantom with spheres.

The volume distribution of the real computed phantom and the results after applying the conventional and the proposed method are summarized in Table 1. It shows the distribution of volume, the porous volume Vp in voxel (vx) and the porosity value P(%).

With small sizes of spheres the two methods give the same results, but with an advanced order in opening, the proposed method gives more precise results than the conventional one. This is explained by the fact that after opening the shape of the component is altered for the conventional method.

2.2.1.2. Phantom with irregular shape. The conventional method of opening (Fig. 7) and the proposed method (Fig. 8) are applied on the compsuted phantom with irregular shape to compare and illustrate the changes that occurs.

The volume distribution of the real computed phantom and the results after applying the conventional and the proposed method are

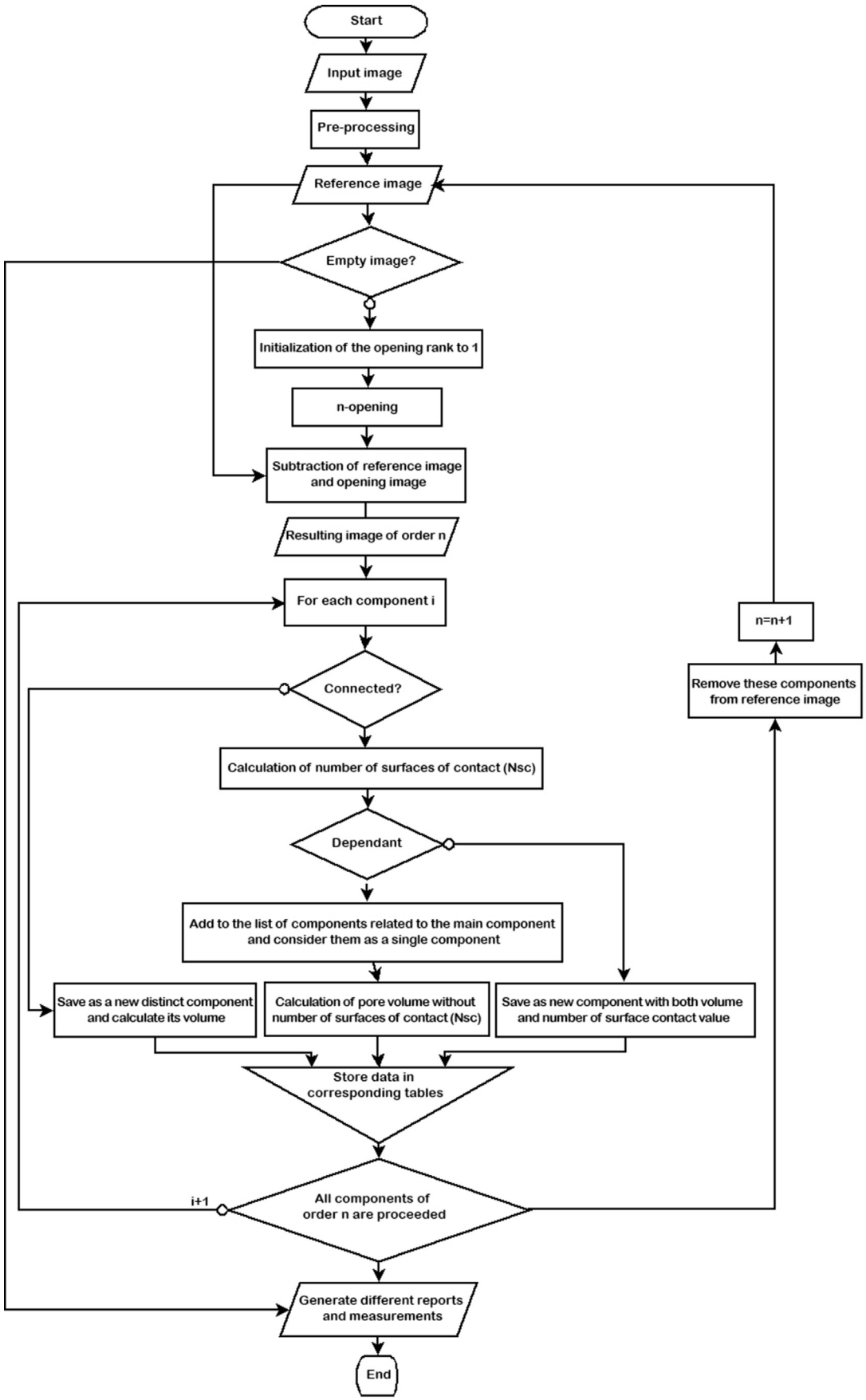

Fig. 5. Flowchart of the proposed method.

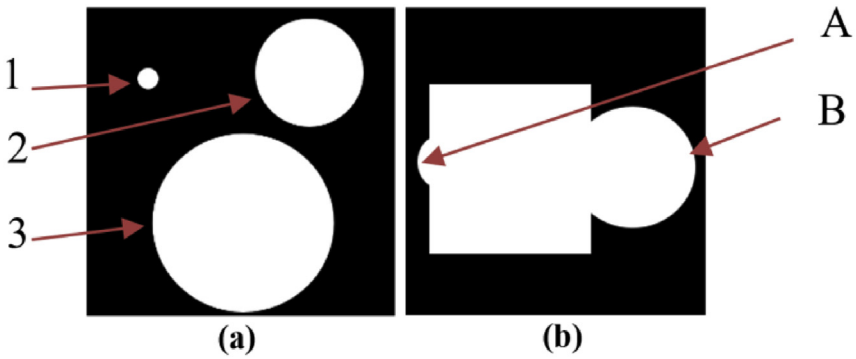

Fig. 6. Computed phantoms with (a) spheres with different sizes (b) irregular shape.

Table 1
The volume distribution (vx) and porosity value (%) of the real computed phantom, the conventional and the proposed method.

Sphere number	The real distribution	Conventional method	Proposed method
1	18612	18612	18612
2	2665234	10145314	2665234
3	12570303	12570303	12570303
Total Vp (vx)	15254149	22734229	15254149
P (%)	79	19	79

summarized in Table 2. It shows the number of component with their volume in voxel (vx).

The difference concerning the number of components for the conventional method is explained by the fact that the component A, we want to keep with the square component, disappears after erosion and cannot be recovered after dilation. The shape of the component B also changes.

The results concerning the proposed method are explained by the fact that after the erosion, the component A disappears but it's recovered after comparing its contact surface with the surface of the adjacent structure. The same principle is applied to the component B, after its dilation, its three corners disappears and thus its initial shape is recovered until it disappears entirely with larger opening. The component B is then omitted, the component A is still remaining and the components shape is preserved.

2.2.2. *Sample studies*

2.2.2.1. SEM image. The overall porosity of the sample, estimated from the apparent density data, is about 80%, which is almost in agreement with the results of the described method applied to the SEM image P = 77%. Table 3 represents the number of pores with their size volume obtained with the SEM image.

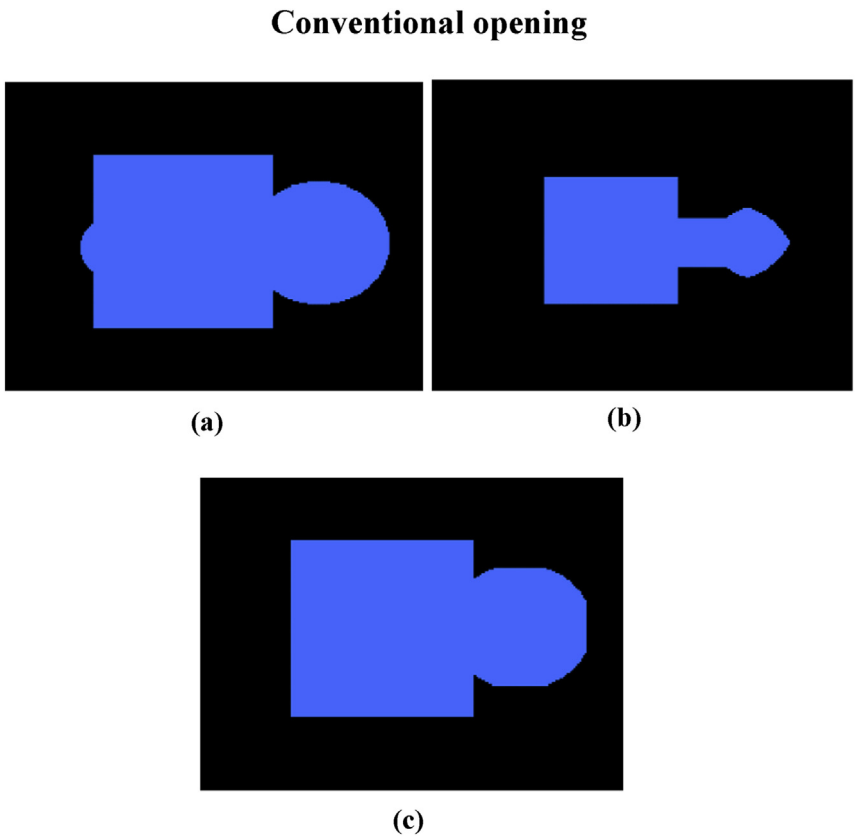

Fig. 7. –Conventional opening:(a) original image (b) image eroded (c) image dilated.

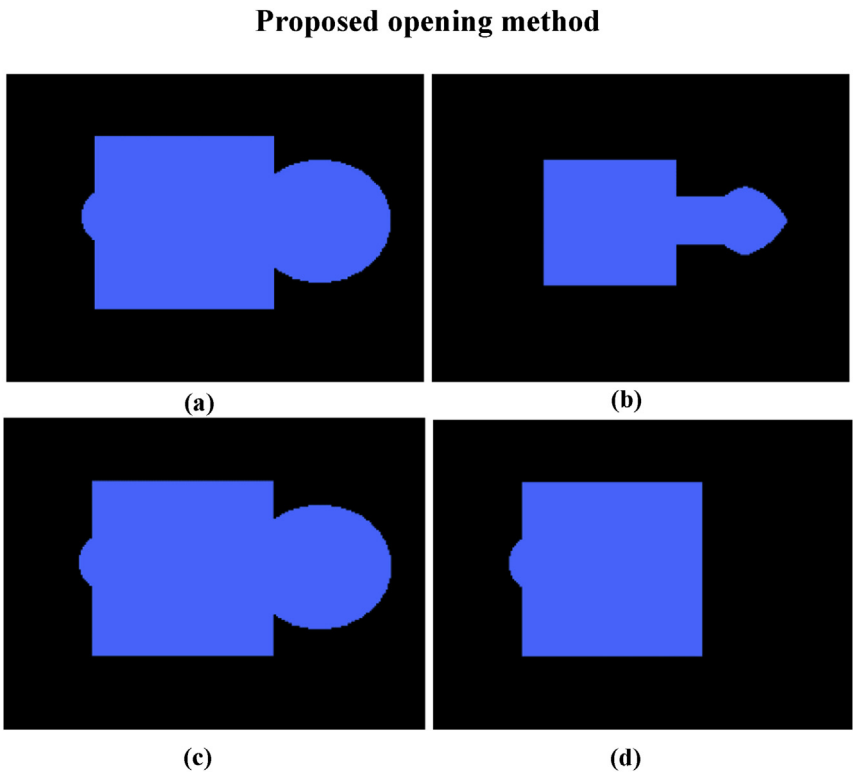

Fig. 8. Proposed method: (a) original image (b) image eroded (c) image after dilated, addition of the small pore on the left and conservaton of the pore shape on the right (d) structure on the right eliminated after opening with raidus larger and small structure still remaning.

Table 2
The volume distribution of the real computed irregular shape phantom, the conventional and the proposed method.

The real distribution		Conventional method		Proposed method	
Component	Volume (vx)	Component	Volume (vx)	Component	Volume (vx)
1	725368	1	11932	1	725368
2	9141261	2	589338	2	9141261
		3	9129218		

2.2.2.2. Tomographic images

2.2.2.2.1. Application of the proposed method. After applying the filtering processing, the proposed method is applied on the X-ray μCT images.

With all the described tools in materials and methods section applied on our μCT images sample, the distribution inside and on the surface of the ceramic of pores with their size volume is obtained (Table 4).

The porosity achieved is about (P) (%) 83% which is almost in line with the overall porosity of the sample, estimated from the apparent density data, (P) (%) 80%.

The results reveal that bio-ceramics have a high volume of porosity (83%) with a high interconnectivity.

The radius variation obtained by the proposed method shows a random distribution of pores inside and on the surface of the ceramic and a wide size variation of pores ranging from 10 μm to 3 mm.

Table 3
Distribution of pores with their size volume of SEM image.

Pore radius size (μm)	$r \leq 30$	$30 \leq r \leq 60$	$60 \leq r$
Number of pores (Nb)	53	26	39
Number of pores (%)	45	22	33
Total Porosity (%)	P = 77		

2.2.2.2.2. Comparison of the conventional and the proposed method applied on μCT images. To know how reliable our method is, the error calculation method was chosen using Eqs. (4) and (5). The results are summarized in Table 5. The manual method was chosen as a reference method for the error calculation.

For a low MAE value, the reliability of the method increases. Compared to the high error value of the conventional method, the error value of the proposed one does not really affect the general statistics. The difference observed in the proposed method is due to the pre-processing step. The result shows that our method gives close outcomes to the real structure.

The proposed method makes it possible to determine the micro and macro porosity and to define with precision the percentage of each class of pores and it helps as well to determine the range of pores sought in such materials.

3. Conclusion

This study concerns the microstructural characterization of porous calcium phosphate bio-ceramics using an adaptive method based on

Table 4
Distribution of pores with their size volume of μCT images.

Pore radius size (μm)	$r \leq 50$	$50 \leq r \leq 100$	$100 \leq r$
Number of pores (Nb)	8350	1460	752
Number of pores (%)	79	13	7
Porosity total (%)	P = 83		

Table 5
MAE value of the conventional and the proposed method for the number of components.

	Conventional method	Proposed method
Mean Absolute Error (MAE)	172	18

mathematical morphology algorithm.

For an efficient quantitative study, the proposed method is used for the separation of the holes, classification and calculation of pore volumes by performing series of openings. This method specifically takes into account, during the computation, the original shape of the structures contrary to the conventional one. Hence, the error calculation caused by the changes of the shape at the component periphery, the problem of the separation of connected pores and the preservation of the irregular shape of the initial pore have been overcame.

The method was evaluated by computerized phantoms. The good performance of the proposed method was demonstrated by comparing the structure distribution on images with the conventional one. The effectiveness and usefulness of the method were demonstrated by its application to SEM and μCT images. This method allows us to have accurate quantitative information of the porous microstructure of ceramic demonstrated through the low error value compared to the conventional one. The results of this work show that the proposed method can have interesting applications in the characterization of porous materials used in the medical field or in other sectors.

Declarations

Author contribution statement

Manal Ezzahmouly: Analyzed and interpreted the data; Wrote the paper.

Abdelmajid Elmoutaouakkil, Mohammed Ed-Dhahraouy: Analyzed and interpreted the data.

Hamza Khallok, Abdelaziz Elouahli: Performed the experiments.

Arnanud Mazurier: Contributed reagents, materials, analysis tools or data.

Abderrazak Elalbani: Contributed reagents, materials, analysis tools or data.

Zineb Hatim: Conceived and designed the experiments.

Funding statement

This research did not receive any specific grant from funding agencies in the public, commercial, or not-for-profit sectors.

Competing interest statement

The authors declare no conflict of interest.

Additional information

No additional information is available for this paper.

References

[1] F.H. Jones, Teeth and bones: application of Surface Science to dental materials and related biomaterials, Surf. Sci. Rep. 42 (2001) 75–205.
[2] M. Bohner, Resorbable biomaterials as bone graft substitutes panel, Mater. Today 13 (2010) 24–30.
[3] X. Yan, C. Yu, X. Zhou, J. Tang, D. Zhao, Highly ordered mesoporous bioactive glasses with superior in vitro bone-forming bioactivities, AngewChemInt Ed. Engl. 43 (2004) 5980–5984.
[4] P. Erlind, B. Lait Kostantinos, P. Gaspare, T. Gianluca, M. Guido, Nano-hydroxyapatite and its applications in preventive, restorative and regenerative dentistry: a review of literature, Ann. Stomatol. 5 (2014) 108–114.
[5] R.Z. LeGeros, Properties of osteoconductive biomaterials: calcium phosphates, Clin. Orthop. 395 (2002) 81–98.
[6] A. JosephNathanael, A. Oyane, M. Nakamura, K. Koga, E. Nishida, S. Tanaka, H. Miyaji, Calcium phosphate coating on dental composite resins by a laser-assisted biomimetic process, Heliyon 4 (2018), e00734.
[7] B. Mueller, Antibacterial active open-porous hydroxyapatite/lysozyme scaffolds suitable as bone graft and depot for localized drug delivery, J. Biomater. Appl. 31 (2017) 1123–1134.
[8] O. Gauthier, J.M. Bouler, E. Aguado, P. Pilet, G. Daculsi, Macroporous biphasic calcium phosphate ceramics: influence of macropore diameter and macroporosity percentage on bone ingrowth, Biomaterials 19 (1998) 1339.
[9] C. Zhongzhong, S. Zhijian, M. Shenggang, W. Xiaoling, L. Zhiying, Biomimetic modeling and three-dimension reconstruction of the artificial bone, Comput. Methods Progr. Biomed. 88 (2007) 123–130.
[10] N. Nain, V. Laxmi, A.K. Jain, R. Agarwal, Morphological edge detection and corner detection algorithm using chain encoding, IPCV 6 (2006) 520–525.
[11] S. Rani, D. Bansal, B. Kaur, Detection of edges using mathematical morphological operators, Open Trans. Inform. Proc. 1 (2014) 17–26.
[12] M. Roushdy, Comparative study of edge detection algorithms applying on the grayscale noisy image using morphological filter, GVIP 6 (2006) 17–23.
[13] J. Serra, Image Analysis and Mathematical Morphology, Academic Press, London, 1982.
[14] G. Matheron, J. Serra, The birth of mathematical morphology, Proc. 6th Intl. Symp. Math. Morphol. (2002) 1–16.
[15] H.J.A.M. Heijmans, Mathematical morphology: a modern approach in image processing based on algebra and geometry, SIAM Rev. 37 (1995) 1–36.
[16] S. Lou, X. Jiang, P.J. Scott, Applications of morphological operations in surface metrology and dimensional metrology, J. Phys. Conf. Ser. 483 (2014), 012020.
[17] S. Beucher, The Watershed Transformation Applied to Image Segmentation, Conference on Signal and Image Processing in Microscopy and Microanalysis, 1991, pp. 299–314.
[18] J. Gauch, Image segmentation and analysis via multiscale gradient watersheds, IEEE Trans. Image Process. 8 (1999) 69–79.
[19] A. Nedzved, S. Ablameyko, I. Pitas, Morphological segmentation of histology cell images, 15th Int.Conf. Pattern Recog. (ICPR'00) 1 (2000) 1500–1504.
[20] L.A. Gee, M.A. Abidi, Segmentation of range images using morphological operations, Rev. Examples 2588 (1995) 734–746.
[21] R. Huang, E. Lum, K.L. Ma, Multi-Scale Morphological Volume Segmentation and Visualization, 6th International Asia-Pacific Symposium on Visualization, 2007, pp. 121–128.
[22] Y. Kimoria, Morphological image processing for quantitative shape analysis of biomedical structures: effective contrast enhancement, J. Synchrotron Radiat. 20 (2013) 848.
[23] E.R. Dougherty, R.A. Lotufo, Hands on Morphological Image Processing, SPIE Publications, Washington, 2003.
[24] J.L. Lacout, Z. Hatim, M.F. Botton, Patent US 6521264 B1, 2003.
[25] J. Goldstein, D. Newbury, D. Joy, C.E. Lyman, P. Echlin, E. Lifshin, L. Sawyer, J. Michael, Scanning Electron Microscopy and X-Ray Microanalysis, Kluwer Academic 1 Plenum Publishers, New York, 2003.
[26] W.A. Kalender, Computed Tomography: Fundamentals, System Technology, Image, Quality, Applications, Wiley, New Jersey, 2005.
[27] E. Maire, J. Buffière, L. Salvo, J.J. Blandin, W. Ludwig, J.M. Létang, On the application of X-ray microtomography in the field of materials science, Adv. Eng. Mater. 3 (2001) 539–546.
[28] K.J. Mortele, J. McTavish, P.R. Ros, Current techniques of computed tomography; helical CT, multidetector CT, and 3D reconstruction, Hepatic Imaging Interv. 6 (2002) 29–52.
[29] T. Sun, Y. Neuvo, Detail-preserving median based filters in image processing, Pattern Recognit. Lett. 15 (1994) 341–347.
[30] N. Otsu, A threshold selection method from gray-level histograms, IEEE Trans. Syst. Man Cybernetics 9 (1979) 62–66.
[31] Z. Fang, M. Yulei, Z. Junpeng, Medical image processing based on mathematical morphology. The 2nd International Conference on Computer Application and System Modeling, Atlantis Press, 2012, pp. 0948–0950.
[32] K. Krishnaveni, A Study on Morphological Watershed Image Segmentation Algorithms and Their Applications to Cervical Cytological Images, Centre for Information Technology and Engineering, 2009 xxiv-212.
[33] B.S. Divakaruni, S.T. Sunkara, Application of Mathematical Morphology to Problems Related to Image Segmentation, the Steering Committee of the World Congress in Computer Science, Computer Engineering and Applied Computing (WorldComp), 2012.
[34] H. HJAM, C. Ronse, The algebraic basis of mathematical morphology I. Dilations and erosions, Comput. Vis. Graph Image Process 50 (1990) 245–295.
[35] C.J. Willmott, K. Matsuura, Advantages of the mean absolute error (MAE) over the root mean square error (RMSE) in assessing average model performance, Clim. Res. 30 (2005) 79–82.